Journal of the Ceramic Society of Japan 124 [10] 1023-1029 2016 Full paper

Processing and characterization of polymer derived SiOC foam with hierarchical porosity by HF etching

Gian Domenico SORARU, Renzo CAMPOSTRINI, Awoke Asmamaw EJIGU, Emanuele ZERA and Prasanta JANA[†]

Department of Industrial Engineering, University of Trento, Via Sommarive 9, 38123 Trento, Italy

A simple process for synthesizing SiOC foams with low density (45–115 kg/m^3) and high porosity (95–98%) is reported here. The process involves the impregnation of a flexible polyurethane foam with a preceramic polymer solution and pyrolysis in the inert atmosphere. SEM analysis showed that the resultant SiOC foam had a fully open interconnected porous structure with dense struts. N_2 adsorption test performed on the as-pyrolyzed SiOC foams showed very low surface area, which can be increased by leaching out the SiO_2-rich network by HF, leaving behind a mesoporous C-rich SiOC foam. The remarkably high surface area up to 147 m^2/g (7350 m^2/liter) has been reached after 24 h etching. HF etching leads to a decrease of the compressive strength. However, a good combination of compressive strength (~80 kPa), porosity (95%) and surface area (7315 m^2/liter) of the foam has been obtained and it makes the SiOC foam a potential candidate for specific applications.

Key-words : SiOC foam, Polymer-derived ceramic, HF etching, Hierarchical porosity

[Received April 4, 2016; Accepted June 7, 2016]

1. Introduction

Open cell ceramic foams, due to their high porosity and large cell size, display high tortuosity coupled with good permeability and low-pressure drops. They are currently employed as filters for gases or liquids. Moreover, owing to the chemical inertness and high-temperature stability of the ceramic materials, ceramic foams can also be used in very aggressive environments and at ultra-high temperatures.

Processing of ceramic foams can be achieved through several approaches:

(i) by the replica method from a polyurethane foam and a ceramic slurry, (ii) by the use of a sacrificial template or (iii) by direct foaming.[1)]

Preceramic polymers are used for the fabrication of advanced ceramics, generally denoted as polymer-derived ceramics (PDCs). Mainly Si-based ceramics of the Si–C, Si–C–N and Si–O–C systems have been studied and reported in the literature from preceramic polymers.[2)]

For the processing of polymer-derived ceramic foam, polyurethane foam replication with preceramic polymer solutions could be simpler and cost effective. However, this method was briefly explored in the early 2000 but soon neglected by the scientific community due to inhomogeneous irregular microstructures reported in the earlier studies.[3)] This method has been recently optimized in our laboratory, to fabricate ceramic foams by direct impregnation of a flexible polyurethane foam with a preceramic polymer. Accordingly, SiC, SiCN and SiOC open cell foams can be produced starting from polycarbosilane, polysilazane and polysiloxane precursors. The advantages of this method, compared to the more conventional replica process (which uses a ceramic slip) is the formation of a dense strut and its lower synthesis temperature.

One drawback of the open cell ceramic foams is their relatively low surface area. Therefore, while the foams are required to perform multifunctional tasks, such as filtration, catalyst, adsorption, extraction, etc., the presence of fine porosity in the ceramic struts may be beneficial. A solution proposed in the literature to achieve this target is by adding a highly porous wash coat to the foam struts.[4)]

Polymer derived SiOC ceramics have been widely studied in the last decade due to their excellent high temperature stability[5)] and novel functional (electrical, optical, chemical) properties.[6)–8)] The amorphous structure of SiOCs has also been the focus of many investigations with the aim of explaining their unusual physical and chemical behavior.[9)–12)] Accordingly, it is now well established that the amorphous SiOC network, formed at low pyrolysis temperatures (1173–1273 K), undergoes a phase separation at higher temperatures (1373–1673 K) leading to the formation of a nanostructure consisting of two interpenetrating networks, one rich in silica and the other one rich in carbon.[9),13)] The phase separated SiOC network, when treated with HF acid develops micro- and meso-porosity. HF dissolves the SiO_2 clusters present in the SiOC nanostructure leaving behind a highly porous C-rich SiOC network.[14)–16)] HF etching study was also performed on the polymer derived SiOC microcellular foams. Specific surface area was increased to one order of magnitude (up to 65 m^2/g) compared to the un-etched samples. This specific surface area was accompanied by micro- and meso-pore formation.[17)]

In the present study, we have used this approach to introduce micro and meso porosity in polymer derived SiOC foams. Accordingly, SiOC open cell foams with cell size 450 μm and with micro-mesoporous struts have been obtained. The SiOC foams have been characterized both from the structural and microstructural point of view. In particular, the specific surface area and the pore volume have been studied by N_2 physisorption. The compressive strength before and after the HF etching treatment has also been investigated.

† Corresponding author: P. Jana; E-mail: prasanta.jana@unitn.it

‡ Preface for this article: DOI http://dx.doi.org/10.2109/jcersj2.124.P10-1

DOI http://dx.doi.org/10.2109/jcersj2.16072

2. Experimental

2.1 Processing of the samples

SiOC ceramic foams (termed as polymer-derived ceramic foams, PDCFs) were prepared following a replica method using polyurethane foam waste (PUFW) and a linear polysiloxane containing Si–H as well as Si–CH_3 moieties as a preceramic polymer. A cyclic siloxane containing allyl groups (Si–CH=CH_2) was used to crosslink the preceramic polymer. Crosslinking was achieved using a Pt catalyst to promote the hydrosilylation reactions between the Si–H moieties and C=C bonds of the crosslinker.[18)]

The preceramic polymer, polyhydridomethylsiloxane, 97% (PHMS) with a molecular weight of ca 1900 and the crosslinker, 2,4,6,8-tetramethyl-2,4,6,8-tetravinylcyclotetrasiloxane, 97% (TMTVS) were purchased from Alfa Aesar (Ward Hill, MA, USA). The platinum catalyst, platinum (0)-1, 3-divnyl-1.2.3.3 tetramethyldisiloxane complex solution in xylene, Pt 2%, was purchased from Sigma-Aldrich (Saint Louis, MO, USA) and diluted with xylene to a more practical 0.1% solution. All chemicals were used as received without any further purification. A flexible polyurethane foam waste (PUFW), collected from University waste basket, normally used for packaging, with ≈50 PPI (pore per inch) was employed in this study.

To prepare the preceramic polymer solution, PHMS and TMTVS were dissolved in acetone using a PHMS:TMTVS = 10:1 weight ratio. The volume of acetone was 1/5 of the volume of the PUFW to be impregnated. This choice ensured that all the solution would be impregnated into the foam pores. The (PHMS+TMTVS):PUFW weight ratio was set to 1:1 and 3:1. Accordingly, two sets of samples were prepared: the 1:1 and the 3:1 samples. The preparation was started by weighing and measuring the volume of the PUFW to be impregnated. Typically 40 mm × 30 mm × 30 mm PUFW parallelepipeds sample was used. Then, the proper amount of PHMS and TMTVS (same as the amount of PUFW for the 1:1 series and 3 times of the amount of the PUFW for the 3:1 series) were added to the acetone and stirred for few minutes. Then the Pt catalyst (200 and 400 μL for the 1:1 and 3:1 series respectively) was added under a gentle argon flow to prevent excess contamination with oxygen and moisture. The impregnation process had been carried out manually by squeezing the flexible PUFW into the solution and releasing it. So that all the solution was sucked into the foam pores. This process was repeated several times until the foam was homogeneously wet and no solution was left in the container. The impregnated foam was left at room temperature for 24 h to allow for the solvent evaporation and then it was pyrolyzed in N_2 flow (150 mL/min) using an alumina tubular furnace (Lindberg Blue, Thermo Fisher Scientific, Waltham, MA USA) up to 1373 and 1573 K. The furnace was purged by flowing N_2 for 5 h before turning on the power. In order to select the proper heating schedule for the processing of the ceramic foams, the behavior during pyrolysis of a sample of PUFW was previously studied. The PUFW heated in N_2 flow showed a maximum decomposition at 763 K and at 1373 K a total weight loss of 97% with a 3 wt% carbon residue. Accordingly, the heating rate was set to 1 K/min with a holding time of 1 h at 673 K (to promote the PUFW decomposition) and 2 h at the maximum temperature (1373 or 1573 K). After the isothermal holding at the maximum temperature, the furnace was switched off and allowed to cool down to room temperature. SiOC foam was obtained. The foam sample was cut using a razor blade into smaller cubic samples for the further processing and analysis. The bulk density was calculated by volume (measured by the dimensions of parallelepiped foams with a digital caliper) and weight (with the help of microbalance) ratio. The resultant SiOC foams were labelled PDCFxT, $x = 1$ for (1:1) and $x = 3$ stands for (3:1) and T stands for temperature at which foams were pyrolysed. For example, SiOC foam prepared with 3:1 and pyrolysed at 1573 K was called as $PDCF_3$1573.

2.2 HF etching

The etching process was performed on cubic PDCF samples. PDCFs were placed in a polyethylene container and 50 ml of a 48% HF solution was added. The samples were left in the solution at room temperature for 1 and 24 h. A magnetic stirrer was not used to prevent damaging the samples and the container was gently shacked manually time-to-time. Then, the etched foams were removed from the HF solution, washed with distilled water and gradually dried in an oven at 308, 343 and 373 K leaving the samples for 24 h at each temperature.

2.3 Characterization

2.3.1 Structural analysis

PDCF was milled in an agate mortar and the powders were used for collecting X-ray diffraction (XRD) spectra with a Rigaku diffractometer (Model D/Max-B, Tokyo, Japan) with Cu Kα monochromatic radiation in a Bragg-Brentano configuration.

Fourier transform infrared spectra (FT-IR) were recorded in attenuated total reflection (ATR) configuration using a Varian 4100 FT-IR Excalibur Series equipment (Lake Forest, CA, USA) in the range 4000–500 cm^{-1}. An average of 32 scans with a resolution of 2 cm^{-1} was recorded on each sample.

2.3.2 Microstructural analysis

The microstructure of the PDCFs was investigated on fracture surfaces using a scanning electron microscope (SEM, JSM-6300F, JEOL, Tokyo, Japan) after sputtering a thin Au film.

Porosity and specific surface area (SSA) of the foams were studied with N_2 physisorption analysis. Adsorption-desorption N_2 isotherms were obtained at 77 K using a Micromeritics ASAP 2010 equipment (Norcross, GA, USA). BET specific surface area was calculated in the interval of $0.05 \leq p/p_0 \leq 0.33$ using a molecular cross sectional area for N_2 of 0.163 nm^2 and a minimum of five data points. The single point total pore volume (TPV) was calculated at $p/p_0 = 0.995$. Pore size distribution was obtained from the desorption branch of the isotherms using the BJH model.

2.3.3 Mechanical property

Compressive strength and young modulus of the PDCFs before and after etching were measured on selected cubic samples (approximately 10 mm × 10 mm × 10 mm) with an INSTRON 4502 machine (High Wycombe, UK) using a deformation rate of 1 mm/min. Two samples from each foam were analyzed for mechanical properties.

3. Results

3.1 PDCF before etching

Figure 1 shows the typical microstructure of the resultant SiOC foams. From the images, the average cell, window and strut sizes were found to be 447, 191 and 40 μm, respectively. The foam exhibits interconnected pores of near hexagonal configuration. The serrated edges of the foam struts are probably formed during the evaporation of the solvent and suggest that the crosslinking of the preceramic polymer was not yet completed. Interestingly, the struts of the SiOC foams are dense as it can be clearly appreciated from the high magnification SEM picture shown in Fig. 1(b). This feature makes the PDCF presented in this paper different from the more conventional ceramic foams

made by the replica method starting from ceramic powders. Indeed, in the latter case, the foam struts are hollow which make the structure weaker.[19),20)]

The linear shrinkage during pyrolysis is ~37%. As expected, PDCF is amorphous in nature up to 1573 K as shown in **Fig. 2**. The values of bulk density are reported in **Table 1**. The density is clearly a function of the initial amount of preceramic polymer used to infiltrate the PUFW and of the maximum pyrolysis temperature. This result can be rationalized considering that PDCF obtained using a (PHMS+TMTVS)/PUFW ratio of 3:1 have thicker struts compared to the samples with a (PHMS+TMTVS)/PUFW ratio of 1:1. At the same time, increasing the temperature from 1373 to 1573 K leads to densification of the amorphous SiOC network with a corresponding increase in density.[21)]

3.2 PDCF after etching

The compositional evolution of the PDCFs during the HF etching process has been followed by FT-IR analysis. The spectra recorded on the $PDCF_3$1373 before and after 1 and 24 h of HF etching are shown in **Fig. 3** and are representative of all the samples. The spectrum of $PDCF_3$1373, before HF etching, shows two main adsorption peaks: the most intense one in the range 1000–1100 cm^{-1} (with a peak position around 1020 cm^{-1}) is assigned to the asymmetric stretching of Si–O bonds while the band in the region 800–900 cm^{-1}, with a peak position around 820 cm^{-1}, can be assigned to the overlapping of Si–C and Si–O vibrations present in mixed C–Si–O sites.[15)] In general, an increase in the number of Si–C bonds in the Si-centered tetrahedra moves the adsorption to higher wavenumbers.[15)] The effect of

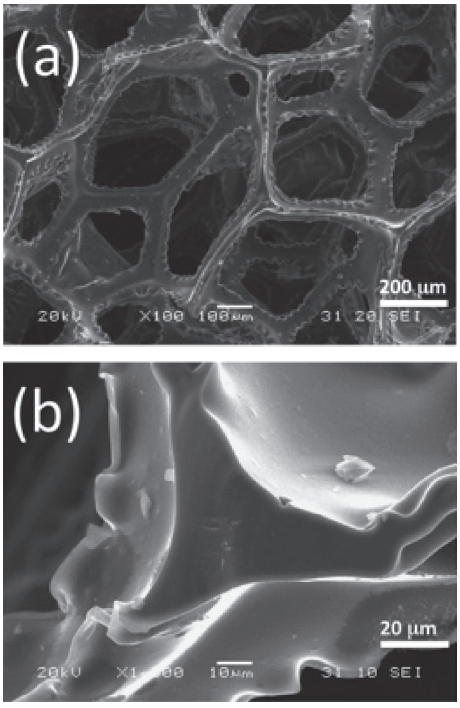

Fig. 1. Typical SEM images of the ceramic foams: (a) microstructure of $PDCF_3$1573 revealing the serrated edges of the struts formed during the solvent evaporation and (b) microstructure of the same sample revealing dense struts.

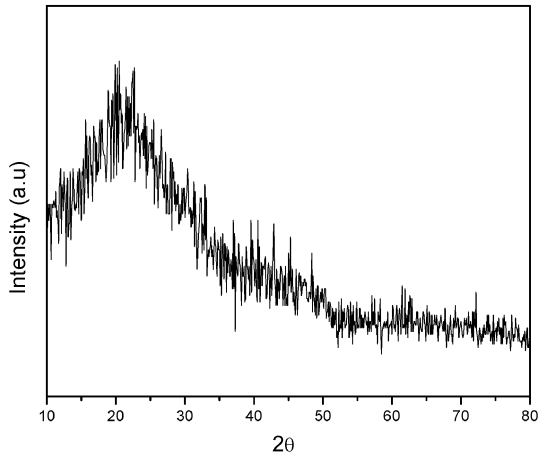

Fig. 2. XRD pattern of $PDCF_1$1573.

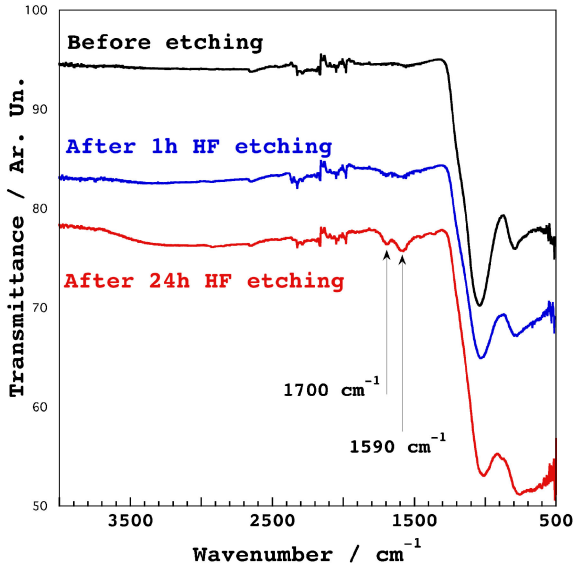

Fig. 3. FT-IR spectra recorded on $PDCF_3$1373 before and after HF etching for 1 and 24 h.

Table 1. Bulk density and porosity values measured on the PDCFs

Samples	(PHMS+TMTVS)/PUFW (kg/kg)	Pyrolysis Temperature (K)	Bulk Density (kg/m^3)	Porosity* (%)
$PDCF_1$1373	1:1	1373	45 ± 5	98
$PDCF_1$1573	1:1	1573	50 ± 5	98
$PDCF_3$1373	3:1	1373	95 ± 5	96
$PDCF_3$1573	3:1	1573	115 ± 5	95

*The porosity (P), has been calculated by the following equation

$$P = 100\,x\left(1 - \frac{bulk\ density}{skeletal\ density}\right)$$

and considering a skeletal density for the SiOC as 2300 kg/m^3.[21)]

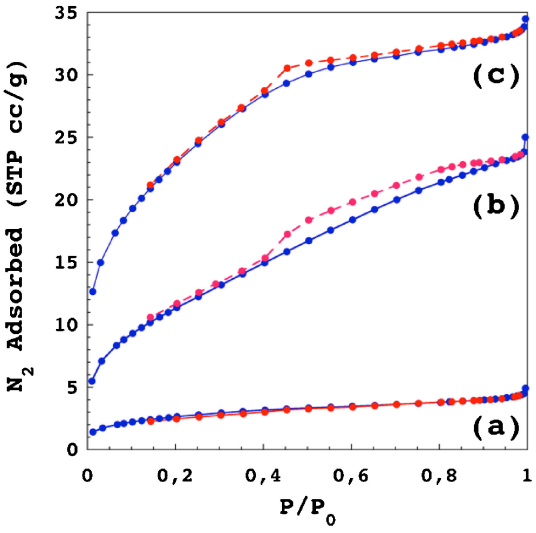

Fig. 4. N_2 adsorption/desorption isotherms of HF etched $PDCF_3$1373 (a) 1 h, (b) 24 h and (c) 24 h etched $PDCF_3$1573.

HF treatments results into a relative decrease of the Si–O band at 1020 cm^{-1} and a corresponding relative increase in the C–Si–O band at 820 cm^{-1}, revealing that, as expected, HF selectively removes the SiO_2-rich phase of the SiOC network.[14)–16)] Indeed, after 24 h of etching, the intensity of the Si–O band at 1020 cm^{-1} has decreased considerable compared to the initial condition and the peak at 820 cm^{-1} is now the most intense one. In addition, two new peaks appear at 1590 and at 1700 cm^{-1}. The band at 1590 cm^{-1} is assigned to C=C bonds of graphitic structures while the vibration at 1700 cm^{-1} could be due to C=O moieties. The absorption at around 1700 cm^{-1}, tentatively assigned to carbonyl groups, has been reported before in HF etched SiOCs[8)] even in conjunction with the band at ~1600 cm^{-1} assigned to graphitic structures.[22)] These findings (the simultaneous presence of the two bands assigned to C=O and graphitic carbon and remembering that ATR technique enhances the contribution of the surface) suggest that: (i) the C=O moieties are connected to the Csp^2 planes rather than with the C atoms bonded to Si atoms in the SiOC network and (ii) the surface created by the HF attack is rich in carbon which is present either as Si–C bonds or as graphitic carbon. Concerning the origin of the carbonyl groups, this is not clear now. One possibility is that they have been formed during the HF etching process. However, their presence in the original SiOC glass cannot be ruled out.

The porosity formed in the PDCFs by HF etching has been evaluated by N_2 physisorption techniques. **Figure 4** shows the absorption-desorption isotherms of HF etched $PDCF_3$1373 and $PDCF_3$1573. The Specific Surface Area (SSA) and Total Pore Volume (TPV) values measured on the samples are reported in **Table 2**.

The starting foams have a negligible surface area as measured by the same technique. HF etching dissolves the silica phase and leaves behind a porous material. The extent of the etching process is a function of the etching time. Comparing samples of the same series and pyrolyzed at the same temperature, it can be noticed that both the SSA and the TPV increase by increasing the etching time. In addition, the data reported in Table 2, indicates that the SSA and TPV increase by increasing the pyrolysis temperature. For example, after 24 h etching, $PDCF_1$1373 and $PDCF_1$1573 displayed SSA 69 and 147 m^2/g, respectively. This result can be rationalized as follows: increasing the maximum pyrolysis temperature promotes the phase separation of the SiOC network leading to a more efficient dissolution of the SiO_2 clusters.[15),23)]

Table 2. SSA and TPV values measured for the PDCFs after HF etching

Sample	Etching time (h)	SSA (m^2/g)	TPV (cm^3/g)
$PDCF_1$1373	1	33	0.026
$PDCF_1$1373	24	69	0.068
$PDCF_1$1573	1	44	0.024
$PDCF_1$1573	24	147	0.068
$PDCF_3$1373	1	8	0.006
$PDCF_3$1373	24	42	0.035
$PDCF_3$1573	1	4	0.002
$PDCF_3$1573	24	81	0.037

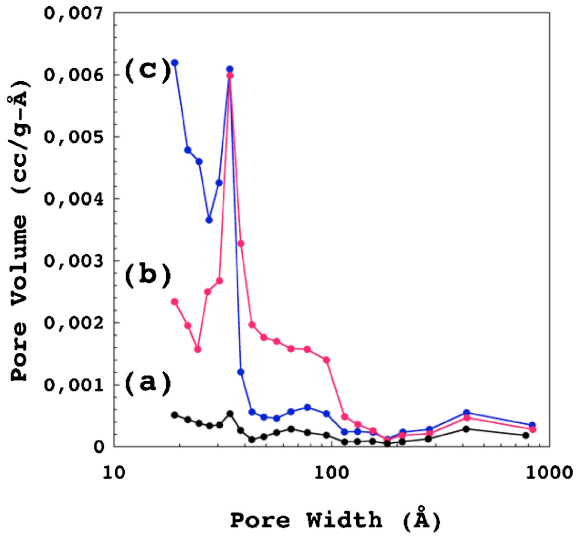

Fig. 5. Pore size distribution curves of HF etched $PDCF_3$1373, (a) 1 h, (b) 24 h and (c) 24 h etched $PDCF_3$1573.

As shown in Fig. 4, the isotherms of the most porous samples are of Type IV, with the hysteresis loop in the 0.4–0.5 P/P_0 range. It clearly reveals the mesoporous features of the etched foams. The corresponding pore size distribution, calculated on the desorption branch of the isotherms, are reported in **Fig. 5**. It reveals the formation of pores with size below 10 nm and with a maximum around 3–4 nm. The foam treated at the highest temperature (1573 K) and etched for 24 h also shows a high fraction of pores smaller than 3 nm.

The microstructure of the HF treated foams was studied by SEM as shown in **Fig. 6**. The HF attack results in the formation of many cracks. Comparing the microstructure of the various HF etched foams, we could not find a clear relation between the etching time or pyrolysis conditions and the number of cracks. The origin of these cracks is not yet clear. Indeed, it is well known that the surface treatment of silicate glasses with HF does not introduce surface cracks but, on the contrary, removes surface defects and increases the fracture strength.[24)] In our understanding, there could be two main reasons for the formation of cracks upon etching. One possibility is that residual tensile stresses, as a result of the pyrolysis process, could be present at the surface of the struts. The dissolution of silica could unbalance the stresses leading to the formation of cracks. A second scenario focuses on the stresses, which build up during drying. It is well known that, while drying a micro-meso porous body such as the one formed by the HF etching SiOC glasses, capillary stresses develop.[25)]

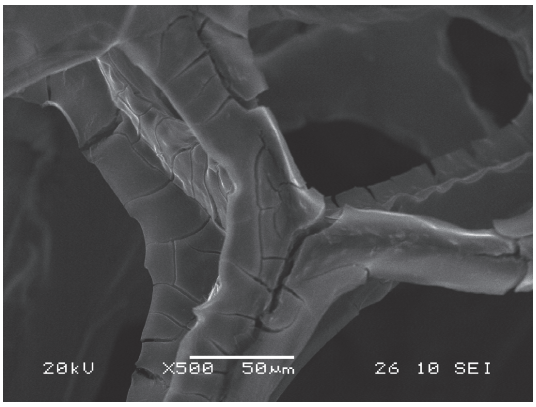

Fig. 6. Typical microstructure of the HF etched $PDCF_1$1373 (etched for 1 h) as revealed by SEM.

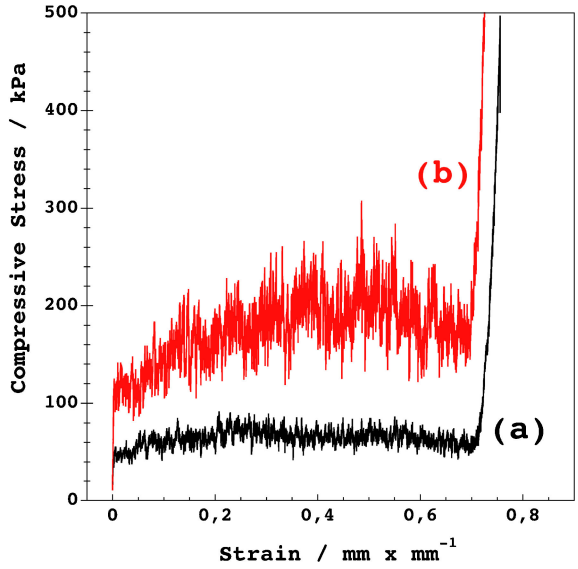

Fig. 7. Compressive stress–strain curve recorded on; (a) $PDCF_1$1373 and (b) $PDCF_3$1373.

The intensity of the drying stresses, according to the Laplace equation, is proportional to (1/r) where r is the pore radius. Since the pore size in the etched PDCFs is of the order of few nm, the intensity of the capillary stresses could be high enough to result in the formation of cracks.

3.3 Mechanical properties

Figure 7 shows the stress–strain compression curve of the sample (a) $PDCF_1$1373 and (b) $PDCF_3$1373. The addition of high amount of polymeric precursor inside the PUFW did not change the typical shape of the curve, characteristic of elastic-brittle foams.[26] Three regions were observed: elastic, collapse and densification. After an initial elastic stage, the stress–strain curve shows a long serrated zone originating from the coexistence of collapsed and uncollapsed regions, typical of foams undergoing successive cell wall fractures. After long serrated zone, densification took place and the stress rose sharply as complete densification begun. As expected, the compressive strength of the $PDCF_3$1373 is higher than $PDCF_1$1373. A maximum value around 200–250 kPa was observed for the $PDCF_3$1373 while for the $PDCF_1$1373 the stress–strain curve has a maximum around 70–80 kPa. On the other hand, the compressive strength seems independent from the maximum pyrolysis temperature as shown in **Fig. 8** where the stress–strain curves for the $PDCF_1$1373 and $PDCF_1$1573 are reported.

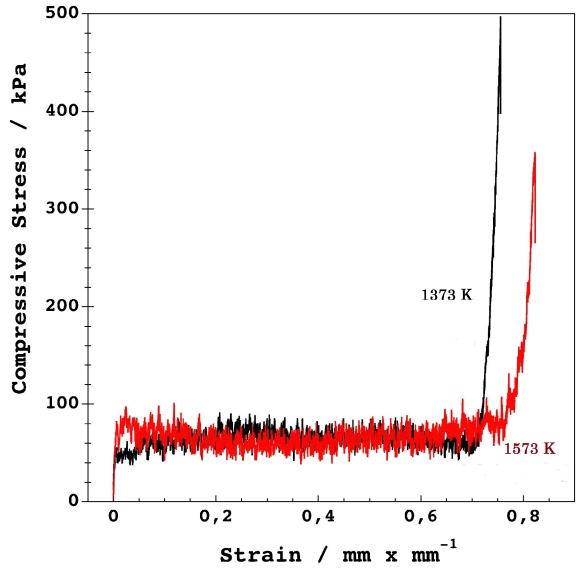

Fig. 8. Compressive stress–strain curve recorded on SiOC foams pyrolyzed at 1373 and 1573 K ($PDCF_1$1373 and $PDCF_1$1573).

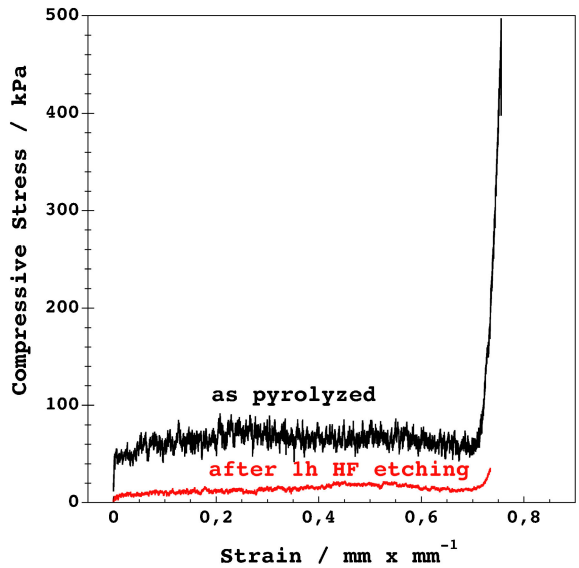

Fig. 9. Compressive stress–strain curve recorded on the $PDCF_1$1373 before and after 1 h of HF etching.

For the $PDCF_1$, HF etching leads to a strong decrease of the compressive strength. After 1 h etching, the compressive strength of the $PDCF_1$ is reduced to 40 kPa (50% reduction) as shown in **Fig. 9**. It becomes non-measurable after 24 h of etching.

The $PDCF_3$ shows a lower decrease of the compressive strength, for example, the $PDCF_3$1573, after 24 h of etching still shows a compressive strength value of 80 kPa as shown in **Fig. 10**.

4. Discussion

According to the processing method reported here, open cell PDCFs with a bulk density in the range 45–115 kg/m^3 and a corresponding porosity of 95–98% can be obtained after pyrolysis at 1373–1573 K. The bulk density can be controlled by the (preceramic polymer)/PUFW ratio and the maximum pyrolysis

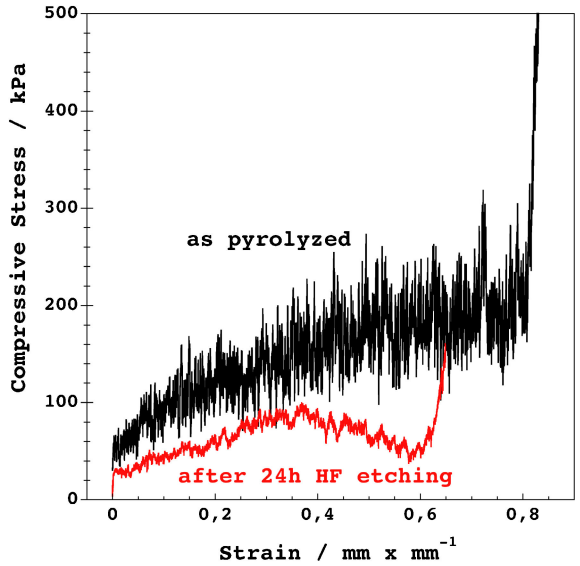

Fig. 10. Compressive stress–strain curves recorded on the $PDCF_3$1573 sample before and after 24 h of etching.

temperature. Increasing the amount of preceramic polymer in the starting solution leads to higher bulk density (due to the formation of ceramic foams with thicker struts) and higher compressive strength. The formation of a dense struts for PDCF is related to the fact that the preceramic polymer, during the impregnation step, does not only coat the surface of the PUFW struts but swells the polymer network. As a result, being the struts non-porous, the specific surface area of the as-pyrolyzed foams is limited to the external surface of the ceramic struts and it is, accordingly, very low. The surface area of the PDCFs can be increased taking advantage of the peculiar nanostructure of the SiOC, which consists of two interpenetrating SiO_2-rich and C-rich networks.[27] The SiO_2-rich phase can be leached out with an HF attach leaving behind a mesoporous C-rich SiOC.

From the N_2 adsorption study, remarkably high value of SSA (147 m^2/g) has been measured for the $PDCF_1$1573 etched for 24 h. Interestingly, the SSA values for the $PDCF_3$ are always lower compared to $PDCF_1$ pyrolyzed in the same condition and with the same time of HF attack. For example, the $PDCF_3$1573 etched for 24 h has a SSA of 81 m^2/g. This result can be rationalized as follows: (i) the average thickness of the struts of the $PDCF_3$ is higher than that of the $PDCF_1$; (ii) for foams pyrolyzed at the same maximum temperature and HF etched for the same length of time, the thickness of the HF etched material at the surface of each strut is the same; (iii) based on these assumptions then the relative amount of etched SiOC, measured as:

$$\frac{grams\ of\ etched\ material}{total\ grams\ of\ material},$$

will be higher for the $PDCF_1$ compared to the $PDCF_3$. On the other hand, for this type of open cell foams, which are often used as filters for liquids or gases, what is more important, is the amount of surface area per unit volume (m^2/liter) of the foam rather than for unit mass. From the known values of bulk density and surface area, the surface area per unit volume (m^2/liter) can be calculated. The bulk density of the etched foams has not been measured so, we can only estimate the surface area per unit volume using the bulk density before HF attack and remembering that, since the HF can dissolve up to ~50% of the mass, the resulting values may be overestimated as a maximum by a factor of ~2. Accordingly, the $PDCF_1$1373 and $PDCF_1$1573 etched for 24 h show surface area 3100 and 7350 m^2/liter, respectively, while $PDCF_3$1373 and $PDCF_3$1573 show surface area 4000 and 7315 m^2/liter, respectively. Another important material property of the foam for potential application is the mechanical strength. From this point of view, the $PDCF_3$1573, etched for 24 h shows a good combination of compressive strength (≈80 kPa), porosity (95%) and surface area (7315 m^2/liter) which makes it a potential candidate for specific applications such as, for example, water filtration and purification.

5. Conclusion

PDCF with very low density (45–115 kg/m^3), high porosity (95–98%) and compressive strength up to 250 kPa was prepared by impregnation of a flexible polyurethane foam with a preceramic polymer solution and pyrolysis in the inert atmosphere.

The (pre ceramic polymer)/PUFW weight ratio used in the impregnation step controls the density and the compression strength of the resultant PDCFs. The PDCF can be etched by HF leading to introduce hierarchical porosity. Remarkably high surface area values up to 147 m^2/g and 7350 m^2/liter have been reached after 24 h of etching for the $PDCF_1$1300 sample. The HF etching leads to a decrease of the compressive strength of the ceramic foams however the $PDCF_3$1573 etched for 24 h shows a good combination of compressive strength (~80 kPa), porosity (95%) and surface area (7315 m^2/liter) which makes it a potential candidate for specific applications.

Acknowledgement This research was made possible through the financial support of the "Fondazione Cassa di Risparmio di Trento e Rovereto" under the contract: Polymer-derived ceramics with hierarchical porosity for water filtration/purification.

References

1) A. R. Studart, U. T. Gonzenbach, E. Tervoort and L. J. Gauckler, *J. Am. Ceram. Soc.*, 89, 1771–1789 (2006).
2) P. Colombo, G. Mera, R. Riedel and G. D. Soraru, *J. Am. Ceram. Soc.*, 93, 1805–1837 (2010).
3) X. Bao, M. R. Nangrejo and M. J. Edirisinghe, *J. Mater. Sci.*, 35, 4365–4372 (2000).
4) A. Zampieri, P. Colombo, G. T. P. Mabande, T. Selvam, W. Schwieger and F. Scheffler, *Adv. Mater.*, 16, 819–823 (2004).
5) A. H. Tavakoli, R. Campostrini, C. Gervais, F. Babonneau, J. Bill, G. D. Sorarù and A. Navrotsky, *J. Am. Ceram. Soc.*, 97, 303–309 (2014).
6) L. Toma, H.-J. Kleebe, M. M. Muller, E. Janssen, R. Riedel, T. Melz and H. Hanselka, *J. Am. Ceram. Soc.*, 95, 1056–1061 (2012).
7) A. Karakuscu, R. Guider, L. Pavesi and G. D. Sorarù, *J. Am. Ceram. Soc.*, 92, 2969–2974 (2009).
8) C. Vakifahmetoglu, M. Buldu, A. Karakuscu, A. Ponzoni, D. Assefa and G. D. Soraru, *J. Eur. Ceram. Soc.*, 35, 4447–4452 (2015).
9) A. Saha, R. Raj and D. L. Williamson, *J. Am. Ceram. Soc.*, 89, 2188–2195 (2006).
10) S. J. Widgeon, S. Sen, G. Mera, E. Ionescu, R. Riedel and A. Navrotsky, *Chem. Mater.*, 22, 6221–6228 (2010).
11) P. Kroll, *J. Mater. Chem.*, 20, 10528–10534 (2010).
12) G. D. Soraru, A. Karakuscu, A. Marquardt, L. Tweeton, P. Dulal and M. Affatigato, *J. Am. Ceram. Soc.*, 95, 3729–3731 (2012).
13) J.-H. Kleebe, C. Turquat and G. D. Soraru, *J. Am. Ceram. Soc.*, 84, 1073–1080 (2001).
14) A. M. Wilson, G. Zank, K. Eguchi, W. Xing, B. Yates and J. R. Dahn, *Chem. Mater.*, 9, 2139–2144 (1997).
15) R. Peña-Alonso, R. Raj and G. D. Soraru, *J. Am. Ceram. Soc.*,

89, 2473–2480 (2006).
16) J. Li, K. Lu, T. Lin and F. Shen, *J. Am. Ceram. Soc.*, 98, 1753–1761 (2015).
17) L. Biasetto, R. Peña-Alonso, G. D. Sorarù and P. Colombo, *Adv. Appl. Ceramics*, 107, 106–110 (2008).
18) Y. Blum, G. D. Sorarù, A. P. Ramaswamy, D. Hui and S. M. Carturan, *J. Am. Ceram. Soc.*, 96, 2785–2792 (2013).
19) P. Colombo, *Phil. Trans. R. Soc. A*, 364, 109–124 (2006).
20) B. Ceron-Nicolat, T. Fey and P. Greil, *Adv. Eng. Mater.*, 12, 884–892 (2010).
21) S. Walter, G. D. Soraru, H. Brequel and S. Enzo, *J. Eur. Ceram. Soc.*, 22, 2389–2400 (2002).
22) F. Kolár, V. Machovic, J. Svıtilová and L. Borecká, *Mater. Chem. Phys.*, 86, 88–98 (2004).
23) G. D. Soraru, R. Pena-Alonso and H.-J. Kleebe, *J. Eur. Ceram. Soc.*, 32, 1751–1757 (2012).
24) R. H. Doremus, "Glass Science", Wiley-Interscience, New York (1994), pp. 156.
25) C. J. Brinker and G. W. Scherer, "Sol-Gel Science: The Physics and Chemistry of Sol-Gel Processing", Academic Press, Inc., New York (1990) pp. 413–418.
26) L. J. Gibson and M. F. Ashby, "Cellular solids. Structure and properties", 2nd Ed. Cambridge (UK): Cambridge University Press (1997).
27) A. Karakuscu, A. Ponzoni, P. R. Aravind, G. Sberveglieri and G. D. Soraru, *J. Am. Ceram. Soc.*, 96, 2366–2369 (2013).